

Ultrafast Deactivation Processes in Aminopyridine Clusters: Excitation Energy Dependence and Isotope Effects

E. Samoylova, V.R. Smith, H.-H. Ritze, W. Radloff, M. Kabelac, and T. Schultz*

Contribution from the Max Born Institute, Max-Born-Str. 2A, D-12489, Berlin-Adlershof, Germany

Received June 1, 2006; E-mail: schultz@mbi-berlin.de

Abstract: Fast excited-state relaxation in H-bonded aminopyridine clusters occurs via hydrogen transfer in the excited state. We used femtosecond pump–probe spectroscopy to characterize the excited-state reaction coordinate. Considerable isotope effects for partially deuterated clusters indicate that H-transfer is the rate-limiting step and validate ab initio calculations in the literature. A nonmonotonous dependence on the excitation energy, however, disagrees with the picture of a simple barrier along the reaction coordinate. An aminopyridine dimer serves as a model for Watson–Crick base pairs, where similar reactions have been predicted by theory.

I. Introduction

The genetic information encoded in DNA is very stable against photochemical damage. By protecting the genetic code against ultraviolet components of sunlight, this photostability may have been an important evolutionary factor. High photostability may be based either on a very rapid excited-state relaxation which is quenching all reactive processes or else on an intrinsic photostability of the excited states. To understand the relevant processes in detail, specific reactive and unreactive pathways were investigated in systems ranging from isolated DNA bases to macromolecular DNA (see ref 1 and references therein). However, the experimental studies are complicated by the extremely short lifetimes of excited states in DNA bases and by the existence of several tautomeric forms of the base pairs. Simple mimetic models of the Watson–Crick base pairs allow an investigation of the basic photochemical reaction mechanisms without these complexities. A famous example is the investigation of double proton transfer in the azaindole dimer.² Here we present results on a particularly suited system, a 2-aminopyridine (AP) dimer, which offers the relevant hydrogen bonds and excited-state reaction pathways to investigate single H-transfer in a simple model system. Figure 1 shows the structure of the AP dimer and the proton-transfer reaction coordinate (N–H distance).

Ab initio calculations characterized the potential energy surface for the lowest locally excited ${}^1\pi\pi^*$ (LE) and charge transfer ${}^1\pi\pi^*$ (CT) states of the planar AP dimer along the intermolecular hydrogen transfer coordinate.³ According to the calculations, an electron transfer from one aminopyridine molecule to the other (LE \rightarrow CT transition) should be followed by a proton transfer along the N–H coordinate, leading to a net hydrogen transfer. At equilibrium geometry, a strong

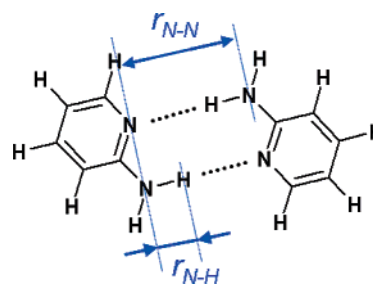


Figure 1. Chemical structure of hydrogen-bound 2-aminopyridine dimer. In the excited state, intermolecular electron–proton transfer occurs along the r_{N-H} coordinate.

coupling of CT and ground state should lead to fast internal conversion and a back H-transfer in the electronic ground state. The electron–proton transfer thus creates a pathway for rapid excited-state relaxation of optically bright electronic states and could quench photochemical reaction channels.

Femtosecond pump–probe spectroscopy⁴ of (AP)_n clusters confirmed the theoretical prediction of fast excited-state relaxation mediated by H-transfer. Upon excitation with 274 nm, the monomer ($n = 1$) and larger clusters $n \geq 4$ show a lifetime of $\tau_1 = 1.5$ ns, equal to the radiative lifetime estimated from high-resolution spectra of the monomer.⁵ The dimer displayed a much shorter lifetime of $\tau_2 = 65$ ps, which was assigned to the H-transfer relaxation channel in the near-planar, doubly hydrogen-bonded structure. For the trimer, both the long-lived τ_1 and the short-lived τ_2 contributions were observed and assigned to different cluster geometries.

Similar H-transfer processes were predicted for the Watson–Crick DNA base pairs guanine–cytosine (GC)⁶ and adenine–

(1) Crespo-Hernandez, C. E.; Cohen, B.; Hare, P. M.; Kohler, B. *Chem. Rev.* **2004**, *104*, 1977.

(2) Douhal, A.; Kim, S. K.; Zewail, A. H. *Nature* **1995**, *378*, 260.

(3) Sobolewski, A. L.; Domcke, W. *Chem. Phys.* **2003**, *294*, 73.

(4) Schultz, T.; Samoylova, E.; Radloff, W.; Hertel, I. V.; Sobolewski, A. L.; Domcke, W. *Science* **2004**, *306*, 1765.

(5) Borst, D. R.; Roscioli, J. R.; Pratt, D. W. *J. Phys. Chem. A* **2002**, *106*, 4022.

(6) Sobolewski, A. L.; Domcke, W.; Hättig, C. *Proc. Natl. Acad. Sci. U.S.A.* **2005**, *102*, 17903.

thymine (AT).⁷ Experimental investigations, however, offered no clear evidence for this process. Time-resolved investigations of the AT base pair in the molecular beam revealed only intramolecular relaxation mechanisms,⁸ but the Watson–Crick base pair might only be a minor component in the molecular beam.^{9,10} Frequency resolved spectroscopy on the GC used chemical substitution to distinguish base pair isomers. Here, a broad spectrum for the WC base pair might be caused by short excited-state lifetimes and reflect ultrafast excited-state relaxation via the H-transfer channel.¹¹

In the present paper, we elucidate the H-transfer mechanism in aminopyridine clusters, investigating isotope effects and the dependence of lifetime τ_2 on the excitation energy. Our goal is to identify the rate determining step along the relaxation pathway, which might be (a) the electronic coupling between LE and CT states, (b) a barrier on the H-transfer coordinate, or (c) the coupling between the CT and ground state. By decreasing the wavelength of the pump pulse starting from a value near the excitation threshold of the $^1\pi\pi^*$ (LE) state of the AP molecule at 299 nm,⁵ we can test how the coupling to the secondary $^1\pi\pi^*$ (CT) state depends on the excess energy in the initially excited $^1\pi\pi^*$ (LE) state. According to the theoretical results of Sobolewski and Domcke,³ a small barrier is expected for the transition between the two states with respect to the proton-transfer coordinate. We probe this barrier by isotopic substitution of the relevant hydrogen atoms in the amino groups with deuterium. We furthermore characterized cluster fragmentation processes, which pose a major problem for the interpretation of our data and for the interpretation of gas-phase cluster studies in general.

II. Experimental Setup

2-Aminopyridine powder (Sigma Aldrich, 99% purity) was evaporated at 60–80 °C and expanded with ~ 1 bar helium into a vacuum chamber. The expansion occurred through the conical nozzle of a pulsed valve (General Valve, series 9) operating at 100–150 Hz. To get narrow or broad cluster distributions, we modified the helium pressure and pulsed valve parameters, such as the opening time and time delay between the gas and the laser pulse. The molecular beam was skimmed and crossed by copropagating pump and probe laser beams in the interaction region of a linear time-of-flight mass spectrometer.

The pump and probe laser pulses were generated by a Ti:Sa oscillator (Tsunami, Spectra Physics, 80 fs pulses at 800 nm) with further regenerative amplification (Spitfire, Spectra Physics). The clusters were excited by the pump pulse at 250, 274, 293, or 296 nm, obtained via an optical parametric amplifier (TOPAS model 4/800/f, Light Conversion) and nonlinear crystals. Photoexcited clusters were then ionized by the probe pulse at 800 nm via a three-photon process. The intensities in the focused pump and probe beams were approximately 0.03×10^{12} and 3×10^{12} W/cm². A motorized translation stage controlled the time delay between the pump and probe pulses within a range of 450 ps. Excited-state dynamics of the clusters were investigated by collecting mass spectra as a function of the pump–probe delay: When the excited-state populations decay, the corresponding ion signals drop proportionally. Signals were accumulated for typically 200 laser pulses at each

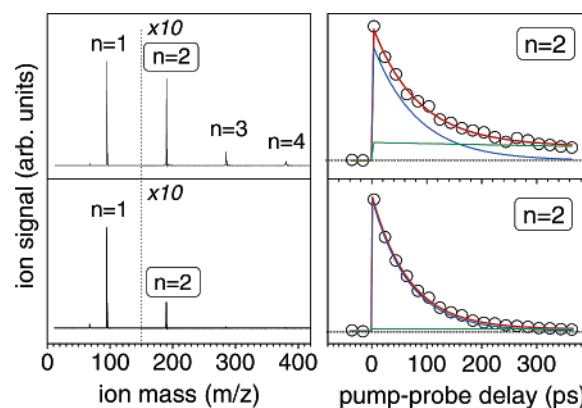


Figure 2. Cluster mass spectra (left) and time-resolved ion signals for the AP dimer (right, \circ) with 293 nm excitation, 800 nm ionization. The spectra differ in the width of the AP_n cluster distribution, but all other experimental parameters were unchanged. A broader cluster distribution ($n = 1-4$, top traces) could be fitted by the sum of two exponential decays (lines) including a long-lived component from the fragmentation of larger clusters. This fragmentation artifact vanished in the very narrow cluster distribution ($n = 1-2$, bottom traces).

delay, and 10 delay scans with alternating scan direction were averaged for a time-resolved mass spectrum. In some delay scans with a range ≥ 300 ps, the ion signals were normalized against toluene to account for small drifts in the spatial overlap of pump and probe beams. Excited-state lifetimes for selected clusters were determined by mono- or biexponential fits, and the corresponding error bars were estimated from multiple measurements.

Deuterated aminopyridine (*N,N*-2D-aminopyridine, DAP) was synthesized by dissolving 2-aminopyridine in a 20-fold excess of deuterated water and removing the solvent in a rotary evaporator. The procedure was repeated three times. Preceding measurements of DAP, we purged the sample lines for 1 h with deuterated water, using a bubbler and helium as the carrier gas. Nevertheless, our mass spectra always showed a small amount of undeuterated and monodeuterated aminopyridine, presumably due to exchange with mobile protons in the sample lines.

III. Experimental Results

We observed considerable fragmentation of larger AP_n cluster ions to smaller AP_{n-x} cluster ions and AP monomers. The ion signals observed for the smaller clusters were therefore contaminated with contributions from larger clusters, and this complicated the interpretation of our data.⁴ We characterized this effect by varying the width of the cluster distribution. The amplitude of fragment signals was proportional to the amplitude of larger cluster signals and could be completely avoided for the AP dimer in very narrow cluster distributions as shown in Figure 2. We therefore minimized the width of the cluster distributions in all experiments, with a natural limitation imposed by the need for reasonable signal amplitudes in the cluster of interest.

In Figure 3 we show the excited-state dynamics for clusters AP_n with $n = 1-3$ for the pump wavelength 293 nm (same as in Figure 2). The trimer signal is a factor of ~ 400 smaller compared to that of the dimer and $\sim 10^4$ with respect to that of the monomer (cf. coordinates in Figure 3). We expect only negligible contributions from fragmentation in this narrow cluster distribution. For the monomer, a monoexponential fit with a 1.5 ns lifetime (corresponding to the known rotational line width⁵) reproduced the experimental decay trace. Due to the limited range of our delay stage, we could not further characterize this decay. The dimer showed a monoexponential

- (7) Perun, S.; Sobolewski, A. L.; Domcke, W. *J. Phys. Chem. A* **2006**, *110*, 9031.
 (8) Samoylova, E.; Lippert, H.; Ullrich, S.; Hertel, I. V.; Radloff, W.; Schultz, T. *J. Am. Chem. Soc.* **2005**, *127*, 1782.
 (9) Kabelac, M.; Hobza, P. *J. Phys. Chem. B* **2001**, *105*, 5804.
 (10) Plützer, C.; Hünig, I.; Kleinermanns, K.; Nir, E.; de Vries, M. S. *ChemPhysChem* **2003**, *4*, 838.
 (11) Abo-Riziq, A.; Grace, L.; Nir, E.; Kabelac, M.; Hobza, P.; de Vries, M. S. *PNAS* **2005**, *102*, 20.

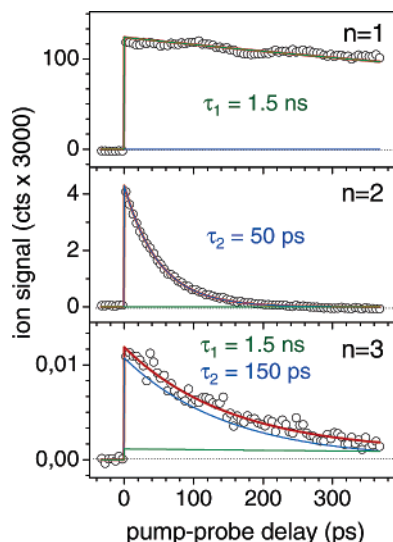


Figure 3. Ion signals of the clusters $(AP)_n$, $n = 1-3$, as a function of the delay time between pump pulses at 293 nm and probe pulses at 800 nm (\circ). The experimental data were reproduced by one or two exponential decays ($-$) with lifetimes of τ_1 and τ_2 .

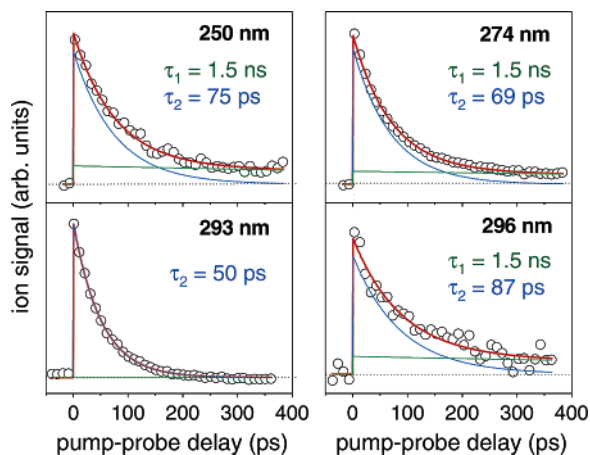


Figure 4. Ion signals (\circ) of the AP dimer as a function of the delay between pump pulses at 250, 274, 293, and 296 nm and probe pulses at 800 nm. Exponential fit curves ($-$) contained two single-exponential contributions with the time constants τ_1 (green) and τ_2 (blue). In all cases, the small τ_1 contributions were proportional to the amount of larger clusters and were assigned to corresponding fragmentation events.

decay with a much shorter 50 ps lifetime, assigned to the theoretically predicted H-transfer pathway.⁴ The interpretation of the noisy trimer signal is ambiguous, but this trace is clearly composed of one or more picosecond components (here we fitted $\tau_2 = 150$ ps) and a long-lived nanosecond component. The dynamics in clusters with $n \geq 4$ resembled the monomer and have been presented previously.⁴

We were particularly interested in the H-transfer dynamics in the AP dimer. We identified the corresponding $\tau_2 < 90$ ps decay at all excitation wavelengths between 250 and 296 nm (Figure 4). In some traces, additional contributions with a longer lifetime $\tau_1 = 1.5$ ns resulted from the fragmentation of clusters with $n \geq 3$ after ionization but did not disturb the determination of the time constant τ_2 . The slowest relaxation rate with a lifetime of $\tau_2 \approx 90$ ps was found for 296 nm excitation (33784 cm^{-1}), close to the origin for the $\pi\pi^*$ transition in the monomer (33549 cm^{-1}). Increased excitation energies led to reduced lifetimes of $\tau_2 = 50-75$ ps, but the shortest lifetime was

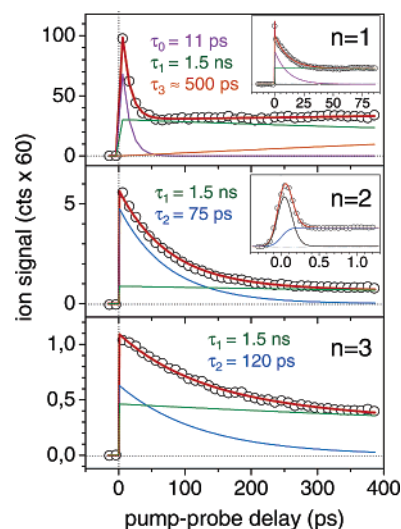


Figure 5. Ion signals (\circ) and fits ($-$) for $(AP)_n$ clusters, $n = 1-3$, as a function of the delay time between pump (250 nm) and probe (800 nm) pulses. All traces showed a short-lived contribution with $\tau \leq 60$ fs, shown with better time resolution for $n = 2$ (inset). The broad cluster distribution shown here (cf. ordinates) illustrates fragmentation effects: The τ_1 components in the monomer and dimer vanish in small cluster distributions and are thus due to the fragmentation of larger clusters. For the monomer, we observed an additional rise with $\tau_3 \approx 500$ ps (orange) due to fragmentation of clusters in the excited state.

observed at 293 nm (34130 cm^{-1}), with moderate excess energies in the excited state.

At 250 nm (40000 cm^{-1}), we excite vibronic states $\sim 6450 \text{ cm}^{-1}$ above the first $\pi\pi^*$ level (Figure 5). All observed cluster sizes $n = 1-5$ showed an additional component with very short lifetime (≤ 50 fs, see inset for $n = 2$), which might be due to ultrafast relaxation of a higher electronic state to the first $\pi\pi^*$ state. For the monomer, the excited-state relaxation occurred with $\tau_0 = 11$ ps and longer-lived contributions were only observed in the presence of clusters (i.e., due to their fragmentation). The high amount of vibrational energy in the $\pi\pi^*$ state is sufficient for cluster fragmentation already in the neutral excited state. This process reduced the excited-state population in the fragmenting cluster and increased the corresponding population in the product channel on the subnanosecond time scale. We observed such fragmentation processes as decay of larger and growth of smaller clusters with additional rate constants. Fragmentation in the neutral is therefore easily distinguished from the ionic fragmentation discussed above, which does not introduce additional rate constants. Fragmentation in the excited state is obvious in the monomer (Figure 5, top), where a rising signal with a time constant of $\tau_3 \approx 500$ ps is caused by fragmentation of excited clusters with $n \geq 2$. The biexponential fit for the trimer (Figure 5, bottom) with lifetimes $\tau_1 = 1.5$ ns and $\tau_2 = 120$ ps may reflect several contributions from distinct cluster structures, as well as the fragmentation processes discussed above.

The isotope effect for the N-deuterated aminopyridine dimer was characterized at pump wavelengths of 250, 293, and 296 nm (Figure 6). Only limited quantities of deuterated substrate were available, which is reflected in the reduced signal-to-noise ratio of the corresponding decay traces. Lifetime τ_2 is on the order of several hundred picoseconds, considerably longer than that in the undeuterated AP dimer. As a result, the distinction between τ_2 and long-lived τ_1 signal components from fragmen-

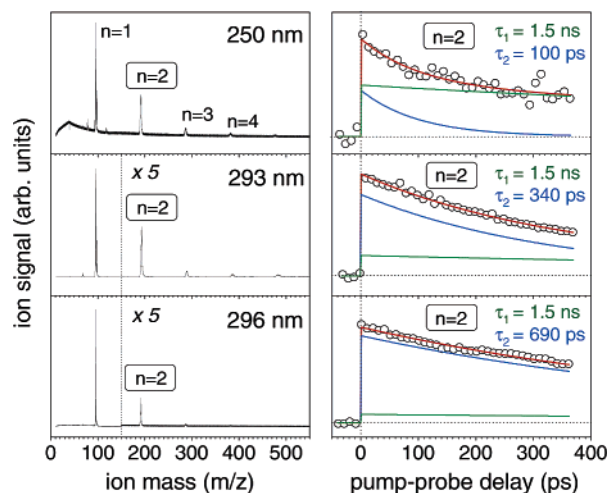


Figure 6. Mass spectra (left) and time-dependent ion signals (○, right) of the deuterated aminopyridine dimer for excitation with 250, 293, and 296 nm and ionization with 800 nm. Contributions from the fragmentation of larger clusters with lifetime τ_1 were proportional to the concentration of larger clusters (AP) $_n$ with $n > 2$ in the mass spectrum.

Table 1. Lifetime τ_2 (H) and τ_2 (D) for Undeuterated and N-Deuterated Aminopyridine Dimers^a

λ_{pump} (nm)	$\bar{\nu}$ (cm ⁻¹)	τ_2^{H} (ps)	τ_2^{D} (ps)	$\tau_2^{\text{D}}/\tau_2^{\text{H}}$
296	33 784	87 ± 20	600 ± 100	6.9
293	34 130	53 ± 5	340 ± 80	6.4
274	36 496	69 ± 10		
250	40 000	75 ± 15	160 ± 50	2.1

^a Errors reflect the range of lifetimes determined in three or more independent measurements.

tation of larger clusters was difficult within the limited range of delay times available in our experiments. This uncertainty resulted in much larger error bounds for the measured lifetimes τ_2 (see Table 1). The magnitude of τ_1 contributions from fragmentation of larger clusters, however, was always in good agreement with the relative amplitude of larger cluster signals in the mass spectra (Figure 6, left). The analysis of the narrow cluster distribution with a weak trimer signal at 296 nm, for example, revealed a small fragment contribution of only $\sim 10\%$ in the dimer signal. The analysis of deuterated monomer species (not shown here) revealed no significant change of the decay time τ_1 , but the accuracy for the determination of these long times is rather low due to the restricted range of delay times.

The measured lifetimes τ_2 of the nondeuterated and deuterated aminopyridine dimer are summarized in Table 1. The wavelength dependence of τ_2 for the nondeuterated dimer was weak and showed a nonmonotonous behavior: the largest values were measured at 296 nm (near the $\pi\pi^*$ (LE) excitation threshold) and at 250 nm (~ 0.8 eV above the threshold). Note the pronounced increase of decay rate for the small change in the excitation wavelength from 293 to 296 nm. The isotope effect for the deuterated AP dimer significantly increased the lifetime τ_2 close to the band origin but was smaller at high excitation energies.

IV. Discussion

According to predictions by ab initio calculations³ and previous results outlined in the introduction, the time constant τ_2 reflects an internal conversion from the initially excited $1\pi\pi^*$ (LE) state to the $1\pi\pi^*$ (CT) state, accompanied by the transfer

of a single H(D) atom. The relatively slow H-transfer rate of 50–90 ps agrees with the predicted reaction barrier for H-transfer. Additionally, the coupling matrix element between the locally excited and charge-transfer state may be small due to a small overlap of the corresponding electronic orbitals, situated on different chromophores.

At first glance, the nonmonotonous wavelength dependence for the H-transfer rate of the nondeuterated dimer does not support the picture of a simple reaction barrier. As we approach and exceed the activation energy another effect must limit the H-transfer rate. One possible explanation may be given by the expected dependence of the reaction barrier on the chromophore distance. Complete structural relaxation of the cluster should occur within the picosecond lifetime of the locally excited state. A fraction of the energy will be redistributed into low-frequency intermolecular modes with highly anharmonic character, e.g., the intermolecular stretch mode characterized by the r_{N-N} distance in Figure 1. Excitation of this mode increases the equilibrium distance between the two aminopyridine chromophores and thus leads to higher H-transfer barriers. Hence, larger vibrational excitation may limit the H-transfer rate, an effect easily imagined in the extrapolated case of having cluster dissociation before the H-transfer occurs.

The large isotope effect $\tau_2(\text{D})/\tau_2(\text{H})$ confirms the existence of a significant barrier for H(D) transfer predicted by Sobolewski and Domcke.³ This isotope effect is largest for small excitation energies, reflecting the respective tunneling rates of H or D atoms through the barrier. At higher excitation energies, the reaction can proceed above the barrier, and we observe a correspondingly smaller isotope effect.

The H-transfer is followed by internal conversion to the ground state and a back-H-transfer reaction. Based on ab initio calculations,³ the lifetime of the $\pi\pi^*$ (CT) state is small (≤ 1 ps). Therefore, the population in the CT state will be small at any time: this state is populated by the slow H-transfer reaction from the locally excited-state and depleted by fast relaxation to the ground state. We conclude, that the corresponding signals are too small to be observed in the time-resolved mass spectra. Photoelectron spectroscopy is sensitive to the electronic state configuration, and we prepare femtosecond electron-ion coincidence experiments in the near future to identify the charge-transfer state spectroscopically.

For the AP trimer, the observed dynamics showed decay rates of $\tau_2 = 100$ – 200 ps and $\tau_1 = 1.5$ ns for the nondeuterated clusters. The dynamics were previously assigned to different cluster isomers, which can or cannot access the hydrogen transfer reaction coordinate.⁴ In Prague, the potential energy surface of the AP trimer was explored using the molecular dynamics/quenching technique (MD/Q)¹² with the Cornell et al. empirical force field (AMBER). The most stable structures were reoptimized using the *Resolution of Identity* MP2 cc-pVDZ basis set with a standard auxiliary basis set. No dominant structure emerged, and the assignment of experimental data to specific structures is therefore difficult. Nevertheless, qualitative features identified with low-level semiempirical methods in the past⁴ were reproduced by our stringent MD/Q calculations: The global minimum of the AP trimer corresponds to a stacked arrangement of two bases with the third base forming a

(12) Molecular dynamics exploration of the configuration space, with subsequent quantum chemical optimization of local minima.

H-bonded bridge in a T-shaped arrangement. This isomer, and others similar to it, may have an unfavorable geometry for H-transfer. In the first local minimum, the doubly H-bonded motif corresponding to the AP dimer is preserved and the third base stands perpendicular. Such structures may be favorable for a H-transfer reaction. Due to the lack of dominant structures, we expect to observe the superposition of many isomers in our experiment which resemble the global and first local minimum. Therefore, despite our best efforts to characterize the trimer decay for this work, we are not able to interpret the relationship between cluster structure and excited-state properties in greater detail.

In conclusion, the experimental study of excited-state dynamics in aminopyridine clusters resulted in a detailed model for an electron–proton transfer reaction (net H-transfer). Our experimental results validate the *ab initio* prediction of a reaction barrier along the H-transfer coordinate.³ The same process may be responsible for fast excited-state relaxation in other hydrogen-bound chromophores, in particular DNA base pairs,⁶ and may offer an explanation for the unstructured absorption of guanine–cytosine Watson–Crick base pairs.¹¹ Other relaxation channels recently identified for DNA bases by experiment and theory involve $n\pi^*$,^{13,14} $\pi\sigma^*$,^{15–17} and $\pi\pi^*$ states.¹⁸ All of those states

are intrinsic to the isolated bases, and their properties do not reflect the specific intermolecular interactions expected for the base pairs. Our results on the H-transfer in a H-bonded dimer model system show that such specific reaction pathways exist and may determine the photochemical properties of biomolecules.

Acknowledgment. We thank Dr. F. Noack for his support by providing the laser system in the femtosecond application laboratory of the Max-Born Institut Berlin. This work was financially supported by the Deutsche Forschungsgemeinschaft through SFB-450, and it was supported by Grant LC512 - Research Project Z40550506 of the Institute of Organic Chemistry and Biochemistry, Academy of Sciences of the Czech Republic.

JA0638612

-
- (13) Broo, A. J. *J. Phys. Chem. A* **1998**, *102*, 526.
(14) Ullrich, S.; Schultz, T.; Zgierski, M. Z.; Stolow, A. *J. Am. Chem. Soc.* **2004**, *126*, 2262.
(15) Sobolewski, A. L.; Domcke, W. *Eur. Phys. J. D* **2002**, *20*, 369.
(16) Pancur, T.; Schwalb, N. K.; Renth, F.; Temps, F. *Chem. Phys.* **2005**, *313*, 199.
(17) Ritze, H.-H.; Lippert, H.; Samoylova, E.; Smith, V. R.; Hertel, I. V.; Radloff, W.; Schultz, T. *J. Chem. Phys.* **2005**, *122*, 224320.
(18) Marian, C. M. *J. Chem. Phys.* **2005**, *122*, 104314.